Copyright © 2015 Tech Science Press FDMP, vol.11, no.4, pp.331-341, 2015

Fluid dynamic analysis of different Yacht configurations with VOF method

R. Savino[1], M. Visone[2], D. Rossetto[3] and V. D'Oriano[4]

Abstract This paper presents two applications of Computational Fluid Dynamics (CFD) to super and mega yacht design, based on the Volume of Fluid method. After an overview of recent literature on the subject, the analysis of the hydrodynamic performances of different hull configurations and of different appendage configurations is presented.

Keywords: Computational fluid dynamics, yacht design, free surface flows.

1 Intoduction

Stern *et al.* (2013) give a detailed review on CFD methods for ship hydrodynamics problems, underlining potentialities but also limitations.

Free surface flows simulations, when rigorously applied, can offer superior results in comparison to traditional water tank or wind tunnel testing. This is particularly applied to high performance racing boats, e.g. for the America's Cup, when the difference between two design candidates can be smaller than the experimental error when running the same towing tank test twice (Viola *et al*, 2012). Numerical simulations eliminate this inconsistency and offer fundamental advantages or complement and integrate physical testing. Simulations may be cheap, fast and reliable because they are run at full scale, eliminating inherent error of scaled test results. Furthermore enhanced flow visualization and force decomposition give designers a much greater understanding of flow phenomena. Limitations of CFD simulations include modeling and numerical errors and their uncertainties should be controlled using rigorous verification and validation. Experimental testing can be the only way to identify CFD limitations and/or to improve the models in view of their validity range extension.

The fluids involved in ship hydrodynamics are water and air, that can be considered as Newtonian fluids. The flow regimes can be considered as incompressible due to usually very low Mach numbers. Therefore, the governing equations for ship flows are the incompressible Navier-Stokes equations. Since typically the Reynolds numbers that

[1] Department of Industrial Engineering, University of Naples "Federico II", Italy.
[2] BLUE Engineering, Italy.
[3] NAET Italia.
[4] Department of Industrial Engineering, University of Naples "Federico II", Italy.

characterize ship hydrodynamics problems are large (order of magnitude 10^7-10^9), the flow is fully turbulent around a large portion of the boat and suitable turbulence models need to be used.

With the continuous growth of computer power and improvement of the numerical models for the solution of partial differential equations, more and more complex ship hydrodynamics problems can be simulated accounting not only for turbulent flows but also for moving domain (e. g. for boat dynamics).

A Direct Numerical Simulation (DNS) of such problems is unaffordable with the computational power available today. Although the Large Eddy Simulation (LES) and the Detached Eddy Simulation (DES) are gaining interest also in the ship hydrodynamics community (Alin *et al.*, 2010), the Reynolds Averaged Navier Stokes equations (RANS) represent the most common approach to solve this kind of problems.

Two main classes of methods for the solution of free surface flows are present in the specialized literature: front capturing methods and front tracking methods.

In the former one phase is simulated, the water, and the boundary of the domain follows the free-surface evolution. The main drawback is that complex free-surface behavior, like spray or overturning waves, cannot evidently be simulated, and the mesh quality can rapidly deteriorate.

Ship hydrodynamics solvers based on these methods are applicable in some applications, since the water phase accounts for most resistance. However, most of them are not capable of solving problems with wave breaking and air entrainment, which have become more and more important due to the development of non-conventional hull shapes and studies of bubbly wake, among others.

By front tracking methods, on the contrary, both air and water are simulated, and the computational domain and mesh are fixed. Both the air and water phases are solved in a coupled manner, which requires treatment of the density and viscosity jump at the interface. An extra variable is introduced so to specify for every cell of the domain whether it belongs to the air or water. The most common methods belonging to this class are the Volume of Fluid (VOF) method and the Level Set (LS) method.

The VOF method is based on a homogeneous approach, where a unique velocity and pressure field is defined for both fluids (Hirt *et al*, 1981). A new variable, called volume fraction of the water f, is defined on the whole domain; f=0 if the element corresponds to an air zone, f=1 if the element corresponds to a water zone and f is a value in the middle if both fluid are present in the cell.

Two-phase solvers are more common in commercial codes such as FLUENT, CFX, STAR-CCM+ (COMET) and open-source CFD solver OpenFOAM, as they are more general tools for a wide range of applications. Ship flow applications are in general performed with high total grid resolution requirements for resolving the air flow besides the water flow. On the other hand, two-phase models are slowly being implemented in specific ship hydrodynamics research codes.

2 Application to yacht design

This paper presents a fluid dynamic analysis based on the Volume of Fluid (VOF) method of different yacht configurations, in the frame of a cooperative research programme between

academy, engineering consulting company and a small shipyard for new yacht development.

Usually super and mega yachts are not designed with highest performance in mind, but the focus is comfort, ease of use and aesthetics while maintaining reasonable hydrodynamic performances.

It has been generally accepted by naval architects that super yachts range from 30 m to 60 m and mega yachts over 60 m.

For luxury motor yachts of 40 to 50 meters, speeds in the range 9-12 m/s (corresponding to Froude numbers of 0.45 to 0.6) are no longer an exception. They must operate at a cruising speed of around 6-8 m/s with a partially submerged transom and the associated drag provides a large portion of the total resistance. Advanced hull designs for the maximum speed are often not efficient and economical at cruising speed and suitable hybrid hull concepts may be investigated to optimize the performances over the entire speed range.

In the present work two applications are considered, i.e. the analysis of the hydrodynamic performances of different hull configurations. In the second part of the paper different appendage configurations are compared to evaluate the influence on the overall yacht performances.

For this purpose the RANS VOF of the commercial code Star-CCM+, CD-adapco, solver with surface tracking capabilities has been validated, comparing numerical with experimental results on a planning hull and then extensively applied to the study cases.

The first study show that this model can be applied to hull design as an experimental test replication (scale 1:1) or in alternative to test for hull (naked or with appendages) moving at steady speed through calm water. Results show free surface tracking capabilities and computations of path lines, lift, drag, trim attitude and sinkage. The trim attitude is defined as the angle between the yacht longitudinal body axis and the waterline.

The second application is an example of optimization of appendages design. In particular flap and interceptor configurations have been studied. Both the appendages are used to adjust the boat longitudinal attitude by means of the lift they generate. Their hydrodynamic performances have been compared, in terms of forces acting on the body, pressure fields and the free surface deformations.

3 Numerical model

The adopted numerical approach is an evolution of the model presented in [29]. Computations have been performed taking into account both flow turbulence and the air-water interface, captured, as explained before, with the Volume of Fluid algorithm. Turbulence has been take into account through the Wilcox k-ω turbulence model (1998). The unsteady RANS and VOF equations have been solved using a sequential algorithm based on the SIMPLE method by Patankar (1980).

A time step of 0.001 s has been chosen in the time implicit algorithm for all the computations, to avoid numerical instabilities associated with the highly nonlinear equations. A further reduction of the time step provides negligible differences.

In order to simulate the relative motion between fluids and body a moving (or non-inertial) reference frame is considered. With a moving reference frame activated, the equations of motion are modified to incorporate the additional acceleration terms occurring due to the change from the stationary to the moving reference frame.

Results of the simulations give the forces and moments on the body surface.

Two degrees of freedom have been taken into account: a vertical movement, corresponding to the hull sinkage, and a rotation around the axis normal to the symmetry plane, that determines the hull attitude.

A global iterative procedure utilizes these results to determine the time-dependent position and orientation of the hull.

This iterative procedure is based on the possibility to dynamically adapt the mesh during the CFD algorithm iterations.

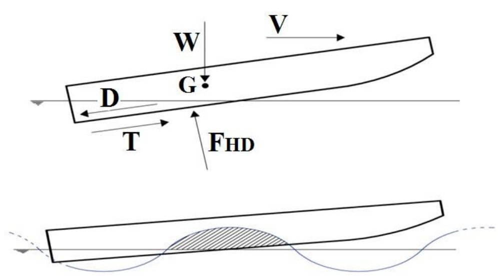

Figure 1: Boat attitude and forces acting in calm water and when waves are present

A Cartesian mesh of approximately 12 million cells has been set up. The grid has been coupled with “matching surface” techniques to join the different blocks.

This procedure allows smaller mesh sizes, faster modeling of complex geometries and a faster dynamical adaption of the mesh, with a computational time cost reduction.

The cell spacing near wall surface has been chosen such that the wall y^+ value does not exceed 10.

A typical example of mesh for one of the configurations investigated in the present paper is shown in Fig. 2.

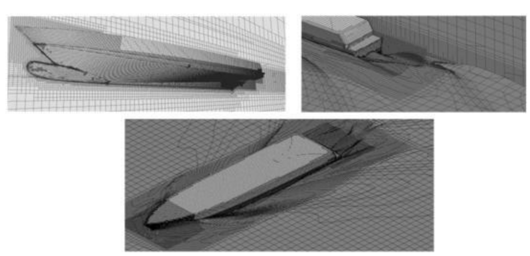

Figure 2: Computational grid for the hull configuration with front bulb

A grid and time step convergence analysis has been carried out.

In particular it has been verified that deviations in results with a finer grid of about 18 million cells, considering forces and moments on the ship, are lower than 2%. Fig. 3 shows a comparison between the generated coarse and fine grids.

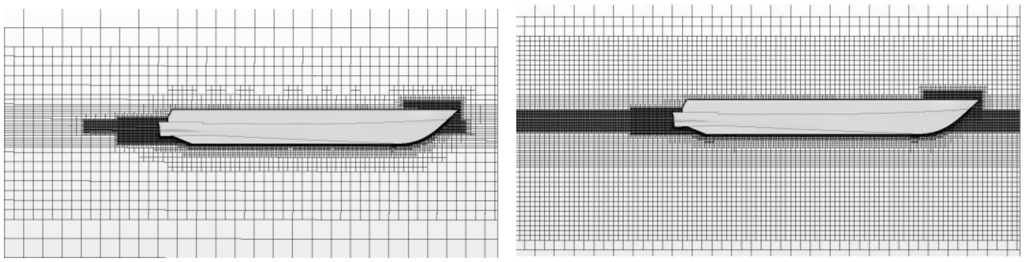

(a) (b)

Figure 3: Coarse (a) and fine (b) computational grid for the naked hull configuration

4 Numerical and experimental results

4.1 Experimental reference test and validation of the model

Validation of the computational simulation has been carried out considering as reference test those already reported in the work of *Visone et al.* (2005), that provides experimental data obtained on scaled hull models at the Brodarski Institute in Zagreb (Fig. 4). Two hulls have been taken into account; the first one with scale ratio 1:3.8 was fully equipped with appendages; the second had scale ratio 1:6.0, naked hull with spray rails.

The same towing condition was simulated in the numerical computation; hulls have been considered to be initially at rest in calm water, and then to move with a relative velocity of 15 m/s for the first Hull and 17.5 m/s for the second one. Lift, drag and dynamic trim have been computed in the final equilibrium positions. The results, in terms of equilibrium position, forces and moments are in good agreement (maximum discrepancy less than 5%) with the available experimental data.

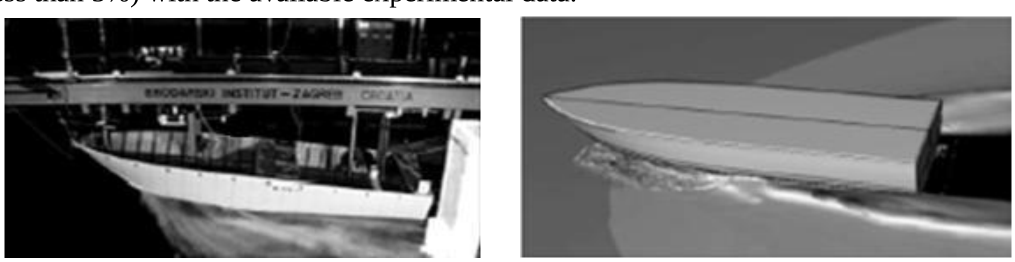

(a) (b)

Figure 4: Free surface shape around the hull; experimental test (a) and computational results (b)

4.2 Hydrodynamic performances of different hull configuration

The hull configurations considered in the study are shown in Fig. 5. The first one is naked

(Fig. 5a), the second one is characterized by a front bulb (Fig. 5b).The length of the boats is 42 m.

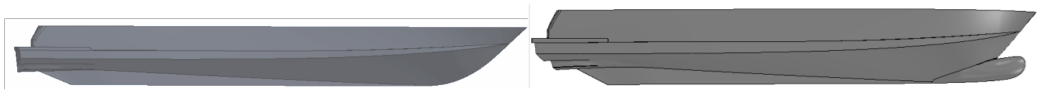

(a) (b)

Figure 5: Hull configurations: naked (a) and bulb (b)

The forces in water include: weight force W, shaft thrust T, drag force D and hydrodynamic force F_H, one static (F_{HS}) and one dynamic (F_{HD}).

Wave runs over the boat and change immersed surface, changing in turn vertical equilibrium, attitude, hydrodynamic and hydrostatic forces.

Operative conditions for the present calculations are:

- Displacement (225 tons)
- Water Line (Z = 2012 mm)
- Velocity: 4.6-6.2-7.7- 9.3-10.8 m/s.

The corresponding Reynolds numbers are, respectively: $9.25x10^7$, $1.23x10^8$, $1.54x10^8$, $1.85x10^8$ and $2.16x10^8$. The corresponding Froude numbers are, respectively: 0.23, 0.31, 0.39, 0.46 and 0.54. Required outputs include: trim, sinkage and drag. Figs. 6~8 show the results for the naked hull configuration at different velocities. The waves profile is shown at the minimum (V=4.6 m/s, Fig. 6a) and maximum (V=10.8 m/s, Fig. 6b) velocities. The corresponding surface pressure distributions are shown in Fig. 7 (a,b).

The maximum pressure occurs at the bottom of the boat, due to the increasing contribute of the hydrostatic pressure at increasing depth. Free surface elevations are illustrated for V=6.2 m/s (Fig. 8a), V=7.7 m/s (Fig. 8b), V=9.3 m/s (Fig. 8c) and V=10.8 m/s (Fig. 8d).

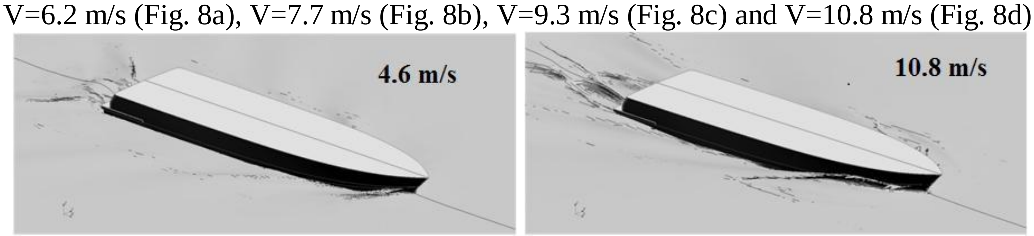

(a) (b)

Figure 6: Waves profile; V=4.6 m/s (a) and V=10.8 m/s (b)

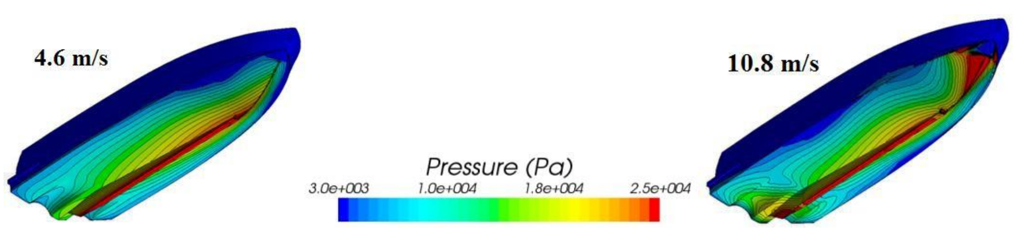

(a) (b)

Figure 7: Surface pressure distribution for the naked hull; V=4.6 m/s (a) and V=10.8 m/s

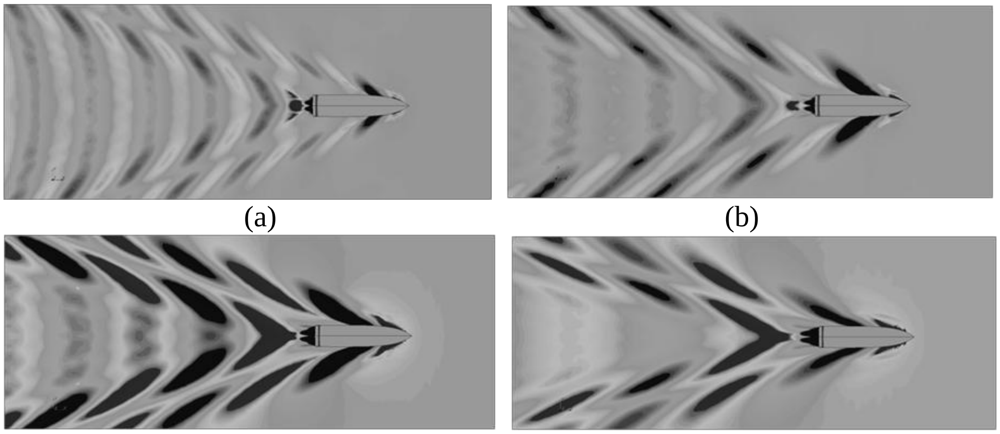

(a) (b)

(c) (d)

Figure 8: Computed surface elevation contours for the naked hull; V= 6.2 m/s (a), V=7.7 m/s (b), V=9.3 m/s (c) and V=10.8 m/s (d)

Fig. 8 shows that as the Froude number increases (increasing the velocity), the wavelength increases while the wavenumber decreases, in agreement with literature. Indeed it is well know that $Fr = \sqrt{\lambda/2\pi L}$, where $\lambda = 2\pi V^2/g$ is the wavelength of the wave propagating with a phase speed equal to V and L is the hull length (Rabaud *et al.*, 2013).

The comparison between the naked and bulb hull configurations is presented in Figs. 9~11. Fig. 9 shows the path lines in the liquid (blue) and in the air (red) phases. The surface pressure distributions are illustrated in Fig. 10.

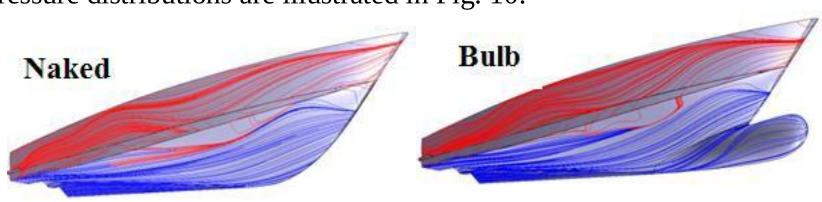

(a) (b)

Figure 9: Path lines distributions on the hull for V=4.6 m/s: naked (a) and bulb (b)

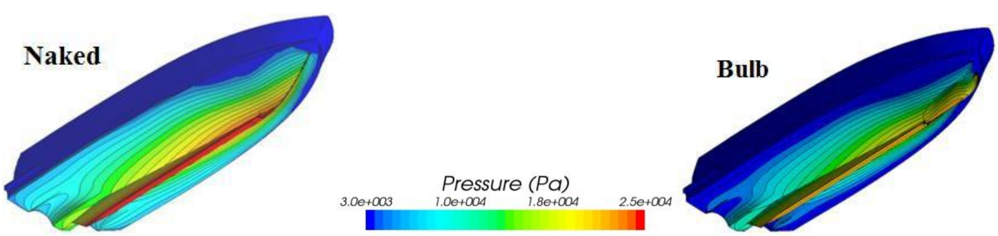

(a) (b)

Figure 10: Surface pressure distribution on the hull for V=4.6 m/s: naked (a) and bulb (b)

It is evident that the maximum bottom pressure is higher for the naked hull configuration. Indeed the bulb hull exhibits better wave breaks properties in the front region of the hull (as shown in Fig. 11), that become better and better increasing the speed.

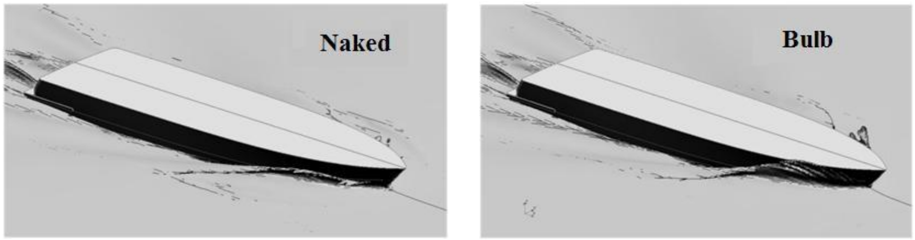

(a) (b)

Figure 11: Waves profile for V=4.6 m/s: naked (a) and bulb (b)

Global computed properties like trim angle, maximum vertical displacement and total drag versus speed are summarized in Fig. 12.

The graphs in Fig. 12 show that, according to the experience, the yacht with a protruding bulb at the bow exhibits a larger trim angle and therefore a larger displacement of the center of mass in vertical direction, compared to the naked configuration. This results in better performances and in wave drag reduction, especially at larger speeds.

Due to the box wave formed immediately before the bow, when the bulb is placed below the water ahead of this wave, water is forced to flow up over the bulb (see also the path-lines in Fig. 9b and Fig. 11b) thereby reducing wave resistance and thus increasing speed range, fuel efficiency and stability.

At the maximum speed (10.8 m/s) the total drag for the bulb configuration is more than 6-7% lower.

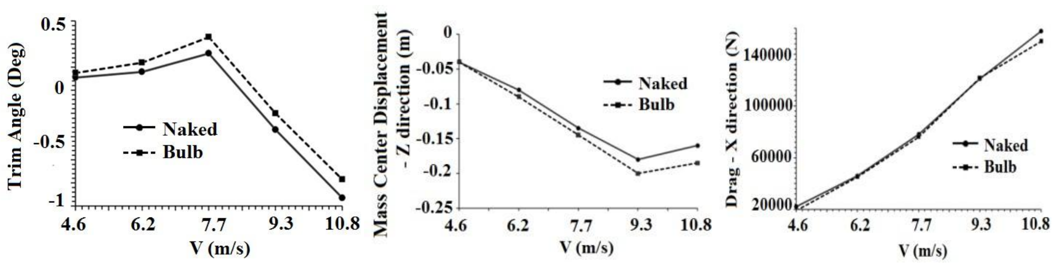

(a) (b) (c)

Figure 12: Trim angle (a), mass center vertical displacement (b) and total drag (c) versus speed for the naked (continuous line) and bulb (dashed line) hull configurations

The most important result is this case is that beyond the global drag values of resistance, the computational fluid dynamics in the comparative analysis allows us to evaluate the sensitivity of basic hydrodynamic parameters, such as drag to motion, with respect to changes in the hull configuration.

4.3 Hydrodynamic performances of different appendages

Another example of application of CFD deals with the sensitivity analysis of the lift and drag force to appendages, providing valuable information in the process of optimization and tuning of them. Two different configurations have been investigated. The same naked considered in the previous paragraph has been analyzed when aft flaps or interceptor are present. The size of the flap and of the interceptor is illustrated in Fig. 13.

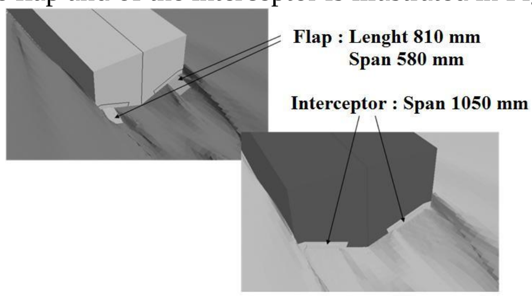

Figure 13: Hull with aft flap and aft interceptor

For this study case the following conditions have been considered:

1) Velocity: 10 m/s. Corresponding Reynolds and Froude numbers are 2.0×10^8 and 0.51, respectively.
2) Flaps angle: 4 °, 8 °, 12 °, 16 °
3) Interceptor prominency: 7mm, 15mm, 30mm, 45mm

The most interesting results are shown in Figs. 14 and 15, where free surface elevation and pressure distributions are illustrated for the two configurations.

In particular, the different color levels in Fig. 14 correspond to the free surface displacements in vertical direction (z=0 is the equilibrium flat see surface).

In Fig. 15 the colors show the scale of the pressure while the isolines correspond to the free surface vertical displacements. Since the interceptor is partially blocking the flow, it is responsible for a wide over-pressure region in the aft area and therefore a larger recovery of the kinetic energy occurs in comparison to the other configuration. This explains why in the case of aft interceptor the lift variation is higher and a more efficient control is possible.

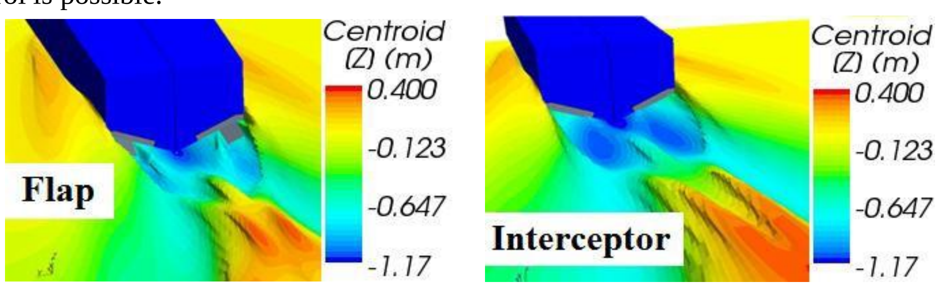

(a) (b)

Figure 14: Free surface elevation contours for the two investigated configurations: hull with aft flap (a) and aft interceptor (b)

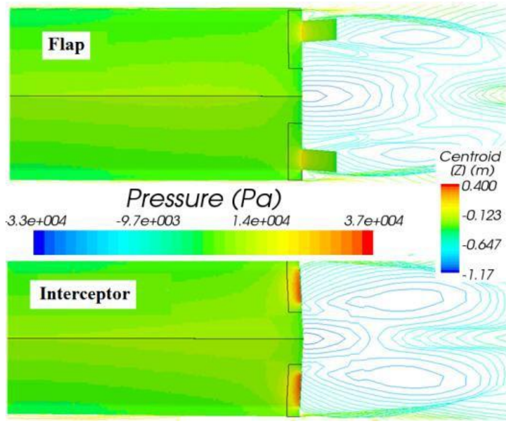

Figure 15: Surface pressure contours for the two investigated configurations: hull with aft flap and aft interceptor

Fig. 16 shows the plot of the drag versus lift increments obtained for the two configurations.
The comparison between the configuration with flaps and interceptors shows that, for trim correction, the latter is more efficient.
In fact, at constant lifting force, the increase of drag due to the flap exceeds that required from the interceptor or, vice versa, at the same drag, the lift generated from the interceptor is superior to that of the flap.
In terms of overall hydrodynamic performance of the yacht, the results show that interceptor can be used more efficiently than conventional outboard flaps at high speed for static or dynamic trim control. The thin plates mounted with sharp tips following the space of the transom edge can be protruded by an actuating system into the water. The discontinuity created by the protruding blade from the transom edge is causing stagnation flow region (characterized by an high pressure, see Fig. 14b and 15b) which modifies the surrounding flow and induces a certain force on the aft bottom. Computational fluid dynamics is able to precisely predict the rather complex hydrodynamic flow field around the interceptors and the distributed parameters (velocity and pressure fields) may be used to evaluate global developed forces in different conditions.

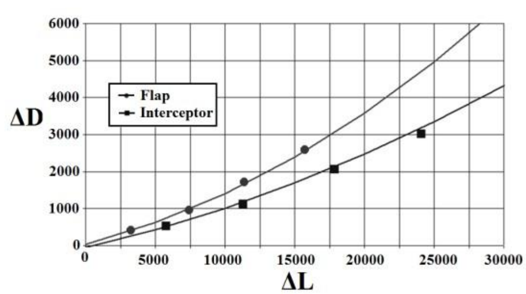

Figure 16: Drag increments versus lift increments (Newton units) for the two investigated configurations

5 Conclusions

The applications presented in this paper show that numerical simulations based on the solution of the Reynolds Averaged Navier-Stokes equations for free surface flows with the VOF method offer very interesting information.

In comparative analysis of different hull configurations sensitivity of basic parameters, such as drag, trim, sinkage, can be quantitatively assessed in a wide range of velocities. Efficiency of different configurations, e.g. with flap or inceptors, can be investigated and the most convenient solution can be selected, according to the performances requirements. Designers may also take advantage from a greater insight into dynamics and flow characteristics. The applications to super and mega yacht design, in the future, can be expected to assess the balance of sailing yachts and the performance differences between design candidates, or the development of boats for hull optimization. More complex designed-oriented computational tools can be further developed for the hull form optimization.

References

Stern, F.; Yang, J. M.; Wang, Z. Y.; Sadat-Hosseini, H.; Mousaviraad, M.; Bhushan, S.; Xing, T (2013): Computational Ship Hydrodynamics: Nowadays and Way Forward. *International shipbuilding Progress*. 60(1-4): 3-105.

Viola, I.M.; Flay, R.G.J.; Ponzini, R. (2012): CFD Analysis of the Hydrodynamic Performance of Two Candidate America's Cup AC33 Hulls. *International Journal of Small Craft Technology*. *Trans. RINA*, 154 (B1), 1 - 12.

Alin, N.; Bensow, R. E.; Fureby, C.; Huuva, T.; Svennberg, U. (2010): Current capabilities of DES and LES for submarines at straight course. *Journal of Ship Research.* 54: pp. 184-196.

Wilcox, D. C. (1998): Turbulence Modeling for CFD. *DCW Industries Inc.*

Patankar, S.V. (1980): Numerical Heat Transfer and Fluid Flow. *Taylor & Francis.* ISBN 978-0-89116-522-4.

Rabaud, M.; Moisy, F (2013): Ship wakes: Kelvin or Mach angle? *Phys. Rev. Lett* 110, 214503.

Hirt, C. W.; Nichols, B. D. (1981): Volume of Fluid (VOF) method for the dynamics of free boundaries. *Journal of Computational Physics.* 39: pp. 201-225.

Visone, M.; Ausonio, C.; Bertetti, P.; Gandolfi, R.; Paterna, D.; Savino, R. (2005): VOF-Dynamic Mesh Simulations of Unsteady Ship Hydrodynamics. *4th International conference on marine hydrodynamics*. Marine CFD, 4; 47-52.